



UNIVERSITY OF LEEDS

This is a repository copy of *The electromotive force in multi-scale flows at high magnetic Reynolds number*.

White Rose Research Online URL for this paper:
<http://eprints.whiterose.ac.uk/89140/>

Version: Accepted Version

Article:

Tobias, SM and Cattaneo, F (2015) The electromotive force in multi-scale flows at high magnetic Reynolds number. *Journal of Plasma Physics*, 81 (6). 395810601. ISSN 0022-3778

<https://doi.org/10.1017/S0022377815001063>

Reuse

Unless indicated otherwise, fulltext items are protected by copyright with all rights reserved. The copyright exception in section 29 of the Copyright, Designs and Patents Act 1988 allows the making of a single copy solely for the purpose of non-commercial research or private study within the limits of fair dealing. The publisher or other rights-holder may allow further reproduction and re-use of this version - refer to the White Rose Research Online record for this item. Where records identify the publisher as the copyright holder, users can verify any specific terms of use on the publisher's website.

Takedown

If you consider content in White Rose Research Online to be in breach of UK law, please notify us by emailing eprints@whiterose.ac.uk including the URL of the record and the reason for the withdrawal request.



eprints@whiterose.ac.uk
<https://eprints.whiterose.ac.uk/>

The Electromotive Force in multi-scale flows at High Magnetic Reynolds Number

STEVEN M. TOBIAS¹†, AND FAUSTO CATTANEO²

¹Department of Applied Mathematics, University of Leeds, Leeds, LS8 1DS, UK

²Department of Astronomy and Astrophysics, 5640 S. Ellis Avenue, University of Chicago, Illinois, 60637

(Received ?; revised ?; accepted ?. - To be entered by editorial office)

Recent advances in dynamo theory have been made by examining the competition between small and large-scale dynamos at high magnetic Reynolds number Rm . Small-scale dynamos rely on the presence of chaotic stretching whilst the generation of large-scale fields occurs in flows lacking reflectional symmetry via a systematic electromotive force (emf). In this paper we discuss how the statistics of the emf (at high Rm) depend on the properties of the multi-scale velocity that is generating it. In particular, we determine that different scales of flow have different contributions to the statistics of the emf, with smaller-scales contributing to the mean without increasing the variance. Moreover we determine when scales in such a flow act independently in their contribution to the emf. We further examine the role of large-scale shear in modifying the emf. We conjecture that the distribution of the emf, and not simply the mean, largely determines the dominant scale of the magnetic field generated by the flow.

PACS codes: (see <http://www.aip.org/pacs/> for the full list of PACS codes)

1. Introduction

It is a great pleasure and privilege to be invited to contribute to this volume in honour of the centenary of the birth of Professor Zel'dovich. Zel'dovich's research interests were so wide-ranging that it is possible to discuss almost any aspect of physics and describe the significant and lasting impact that he had on that field. We shall not even attempt to describe the breadth of the contributions and deep insight of Professor Zel'dovich's research since this has been noted repeatedly both by scientists and historians of science (Sunyaev 2004; Hargittai 2013), nor shall we review one of the many fields to which Zel'dovich made such telling contributions. Rather we shall describe a new investigation that brings together two of Professor Zel'dovich's research interests, random flows in magnetohydrodynamics and dynamo theory.

An understanding and categorisation of the dynamo properties of turbulent flows can only emerge with the recognition that turbulent flows exist as a superposition of coherent and random structures. The ratio of the importance of each of these classes of flow to the dynamo properties depends on the physical setting of the flow. In general for astrophysical and geophysical flows, the interaction of rotation and stratification leads to the enhanced importance of coherent structures (see e.g. Tobias & Cattaneo 2008*a*). This typically involves long-lived structures — by which we mean structures with a coherence

† Email address for correspondence: smt@maths.leeds.ac.uk

time longer than their turnover time — contributing significantly to the generation of magnetic fields.

Dynamo theory has traditionally been separated into two distinct approaches. The first, often termed “Small-scale dynamo theory” or “Fluctuation dynamo theory” examines whether and how fluid flows can act so as to sustain magnetic fields on scales smaller than or up to the typical scale of the energy containing eddies. Despite the irritating presence of anti-dynamo theorems, which rule out the possibility of dynamo action if either the fluid flow or the magnetic field possesses too much symmetry, it has now been established that sufficiently turbulent flows at high enough magnetic Reynolds number (Rm) are almost guaranteed to act as small-scale dynamos (Vainshtein & Kichatinov 1986; Finn & Ott 1988; Galloway & Proctor 1992; Childress & Gilbert 1995). At this point it is worth noting that the two most famous and irritating theorems that dynamos must circumvent are Cowling’s Theorem (Cowling 1933), which prescribes the possibility of an axisymmetric *magnetic field* being generated by dynamo action, and Zel’dovich’s Theorem (Zel’dovich 1957) which rules out two-dimensional flows (i.e. flows possessing only two components) as dynamos. Much ingenuity has been brought to bear in determining simple flows that are able to circumvent the strictures of Zel’dovich’s Theorem; in this paper we will be utilising a class of flows (so-called $2\frac{1}{2}$ dimensional flows) that *are* able to produce dynamos and are amenable to computation at high Rm .

The second approach termed “Large-scale dynamo theory” (Steenbeck *et al.* 1966; Moffatt 1978; Krause & Raedler 1980; Brandenburg & Subramanian 2005) is utilised to describe how systematic magnetic fields can emerge on scales larger than the turbulent eddies. It is this theory that is often used to describe the dynamics of astrophysical magnetic fields such as those found in planets, stars and galaxies. Indeed the eleven-year solar cycle, in which the global magnetic field of the Sun waxes and wanes, with magnetic waves travelling from mid-latitudes towards the equator as the cycle progresses, is attributed to the action of a large-scale dynamo. Large-scale dynamos are subject to the same anti-dynamo theorems as small-scale dynamos (no assumption about the scale of the field is made in either Cowling’s or Zel’dovich’s Theorems) and so the utilisation of similar ingenious tricks as those brought to bear for small-scale dynamos (see e.g. Roberts 1972) may prove particularly useful.

The role of the turbulent cascade in both small and large-scale dynamo theory has been extensively studied and a complete review is well beyond the scope of this article. In many cases multi-scale flows are driven by a forcing at moderate scales in a system at high fluids Reynolds numbers. The importance of inertia at high Re usually leads to the formation of a turbulent cascade and the emergence of a statistically stationary flow that exists on a large range of spatial scales (i.e. a multi-scale flow). This is a nice procedure since the properties of the flow can be changed by the addition of rotation or stratification or modification of the forcing. However in this set-up it is extremely difficult to retain precise control of the properties of the turbulent cascade (for example the spectral-slope of the flow, the correlation time of the eddies and the (scale-dependent) degree of helicity of the flow.) Another popular setting for examining turbulent dynamo action is that where the flow is driven by thermal driving leading to convection, either in plane layers or spherical shells (Tobias *et al.* 2008; Käpylä *et al.* 2010; Augustson *et al.* 2014). These are natural systems to study owing to their importance in geophysical and astrophysical fluids. However here energy input occurs on a range of spatial and temporal scales and control over the properties of the turbulent cascade is even more difficult than for driven flows. Categorising the properties of the spectra of such turbulent flows (both forced and convective) is the focus of much ongoing research and we do not pursue this further in this article.

Rather we take the view that for the kinematic dynamo problem, more control can be exerted by prescribing the form of the flow, rather than that of the driving. This technique has been utilised successfully in determining what flow properties are essential for dynamo action and indeed for dynamo action at high Rm . Statistical theories, such as those close to the heart of Zel'dovich, have also led to the characterisation of the dynamo properties of flows with zero or short correlation times; for a review see Tobias *et al.* (2011). It has been demonstrated, *inter alia* that these random flows can act as dynamos (even when the magnetic field dissipates in the inertial range of the turbulence — the so-called low-Pm problem), and may produce large-scale fields if the flow lacks reflectional symmetry (although these will be subdominant to fields generated on the resistive scale Boldyrev *et al.* (2005)).

The competition between coherent structures and random flows in generating small-scale magnetic fields has been systematically studied in a series of papers (Cattaneo & Tobias 2005; Tobias & Cattaneo 2008*b*). It has been shown that the presence of coherence in space and time can overcome the randomness and lead to systematically enhanced small-scale dynamo action. Furthermore, the small-scale dynamo properties of a multi-scale flow that is dominated by coherent (in time) structures has been elucidated; the slope of the spectrum was shown to play a key role in determining the velocity scale responsible for dynamo action. Here a competition between the local (i.e. at spatial scale $1/k$) magnetic Reynolds number ($Rm(k)$) and turnover time ($\tau(k)$) selects the eddy-scale responsible generating small-scale magnetic fields; hereinafter we term this scale the “dynamo scale”. The application of this theory to a multi-scale flow enables the calculation of the expected growth-time of the small-scale field, as comparable with the turnover time of the “dynamo eddy”.

Of course, for flows lacking reflectional symmetry, this small-scale dynamo must compete with that generating systematic large-scale fields; and compete it does — extremely effectively. In general, unless some process such as diffusion, shear-suppression or nonlinearity acts so as to suppress the small-scale dynamo, it will outperform the large-scale dynamo[†]. At high Rm diffusion is not really a viable mechanism for this suppression and so shear and nonlinear effects remain as the prime candidates. In this paper, we shall not focus on this competition, although we shall return to this important consideration in the discussion. Rather we shall examine the contribution to large-scale field generation (via the electromotive force) of different scales in a multi-scale flow. Once these contributions have been characterised then a complete theory of the competition between large and small-scale dynamos is possible.

In the next section we shall describe the general model problem of the calculation of the electromotive force (emf) in $2\frac{1}{2}$ dimensional flows and review previous findings for flows on one scale; we shall conclude the section by generalising the set-up to include a flow on a range of spatial scales. We shall argue that, although the mean emf is important in determining the large-scale dynamo properties, higher moments of the distribution (for example the variance of the emf) may determine whether the large-scale mode is ever seen. In Section 3.2 we determine under what circumstances scales in the flow act independently of each other by determining the distributions of the emf for flows at different spatial scales. We then calculate the moments of the distribution of the emf as a function of large-scale shear rate (for a variety of flows with differing ranges of spatial scales and correlation times) and construct parameterisations of the effect of shear on the distribution of the emf. We conclude in the discussion by postulating how our understanding of the factors controlling large- and small-scale dynamo action may

[†] This was termed the “Suppression Principle” by Cattaneo & Tobias (2014)

be used to determine *a priori* whether a given flow will lead kinematically to a large or small-scale dynamo.

2. Formulation

As for the dynamo calculations of Tobias & Cattaneo (2013); Cattaneo & Tobias (2014), we consider a flow for which the basic building block is a cellular flow, with a well-defined characteristic scale and turnover time. In addition, it is useful to consider flows for which the electromotive force (emf) can be unambiguously measured. We therefore utilise the circularly polarised incompressible Galloway-Proctor flow at scale k first introduced by Cattaneo & Tobias (2005). We take Cartesian co-ordinates (x, y, z) on a 2π -periodic domain, and consider a flow of the form

$$\mathbf{u}_k = A_k (\partial_y \psi_k, -\partial_x \psi_k, k\psi_k), \quad (2.1)$$

where

$$\psi_k(x, y, t) = (\sin k((x - \xi_k) + \cos \omega_k t) + \cos k((y - \eta_k) + \sin \omega_k t)). \quad (2.2)$$

This 2.5-dimensional flow is maximally helical, taking the form of an infinite array of clockwise and anti-clockwise rotating helices such that the origin of the pattern itself rotates in a circle with frequency ω_k . Here A_k is an amplitude and ξ_k and η_k are offsets that can be varied so as to decorrelate the pattern, and therefore control the degree of helicity. Here they are random constants that are reset every τ_d , which can therefore be regarded as a decorrelation time. In this paper we only consider the case where $\xi_k = \eta_k$ and the flow remains maximally helical.

The dynamo properties of this type of flow acting at one scale are well-understood, (Cattaneo & Tobias 2005), and so are the inductive properties as measured by the emf (Roberts 1972; Plunian & Rädler 2002; Courvoisier & Kim 2009; Courvoisier *et al.* 2006). Because the velocity does not depend on the z co-ordinate, the electromotive force can easily be measured by applying a z -independent mean field $(B_0, 0, 0)$ and measuring the resulting emf $\mathcal{E} = \langle \mathbf{u}' \times \mathbf{b}' \rangle$ where the angle brackets denotes an average over horizontal planes (Roberts 1972).

In this paper we wish to calculate the large-scale induction of a superposition of these flows and therefore set A_k and ω_k at each scale k . We are free to choose A_k to mimic the properties of any spectrum of turbulence. Having chosen A_k there is then a unique choice of ω_k such that the associated dynamo action at scale k has the same asymptotic growth-rate measured in units of the local turnover time (see e.g. Cattaneo & Tobias 2005). With this choice all of these cells look the same at their own scale. The combined cellular flow takes the form of a superposition of these flows on scales between k_{min} and k_{max} , i.e. we set

$$\mathbf{u}_c = \sum_{k_{min}}^{k_{max}} \mathbf{u}_k, \quad (2.3)$$

where k_{min} and k_{max} control the range of scales of the multi-cellular flow.

As in Tobias & Cattaneo (2013) we set $A(k) = k^{-4/3}$ and so $\omega_k = k^{2/3}$ and the decorrelation time $\tau_d = \tau_0 k^{-2/3}$. With these scalings the turnover time $\tau_k \sim 1/\omega_k$ and the magnetic Reynolds number $Rm(k) \sim A(k)/\eta$ are given by (Tobias & Cattaneo 2008a)

$$\tau_k \sim k^{-2/3}, \quad (2.4)$$

$$Rm(k) \sim k^{-4/3}. \quad (2.5)$$

We stress here that we have not attempted to model the scale-dependence of the kinetic

Run	k_{min}	k_{max}	τ_0
A	8	20	0.1
B	8	40	0.1
C	8	100	0.1
D	21	40	0.1
E	41	100	0.1
F	8	20	2.0
G	8	40	2.0
H	8	100	2.0
I	21	40	2.0
J	41	100	2.0

TABLE 1. Caption: All integrations are carried out with $\eta = 10^{-4}$

helicity for the multi-scale flow. We believe that this is dependent not only on the form and scale of the driving mechanisms, but also the prevailing conditions (i.e. rotation rate, stratification and the presence or absence of large-scale shear.) This will be investigated in a forthcoming paper.

To this multi-cellular flow we may add a steady unidirectional large-scale shear of the form

$$\mathbf{u}_s = (V_0 \sin y, 0, 0). \quad (2.6)$$

For this prescribed flow $\mathbf{u} = \mathbf{u}_s + \mathbf{u}_c$ and a given B_0 (and selected k_{min} , k_{max} and V_0) we solve the linear inhomogeneous induction equation. The equations are integrated until the emf has reached a statistically steady state — this is achieved as in this two-dimensional system, where the magnetic field does not depend on z , no dynamo action is possible — though of course dynamo action is possible if solutions with a finite vertical wavenumber are allowed (Tobias & Cattaneo 2013).

3. Results

3.1. Electromotive force for flows at different scales

As noted in the previous section, the electromotive force is calculated for an imposed constant mean magnetic field in the x -direction. As this is the direction in which the shear is imposed it only makes sense to measure the x -component of the emf \mathcal{E}_x . Henceforth in this paper we refer to this as the emf \mathcal{E} . We consider the kinematic regime where the back-reaction of the magnetic field on the flow is negligible.

The flows we integrate are summarised in table 1. We consider flows with a range of spatial scales, with some (e.g. flows A and F) only having energy at large scales, some (e.g. flows E and J) only having energy at smaller scales and some (e.g. flows C and H) having energy at a wide range of spatial scales. In addition some of the flows we consider are formed by adding together more restricted flows; for example flow B is the sum of flows A and D (likewise $G = F + I$) whilst flow H is the sum of flows B and E (likewise $H = G + J$). These constructions will be used to examine whether the spatial scales act independently in generating the emf. Furthermore flows A–E are at short correlation time, whilst for flows F–J the correlation time of the eddies at scale k is comparable to their turnover time at that scale. These flows are considered in the absence and presence of large-scale systematic shears of various strengths. Henceforth we utilise the shorthand

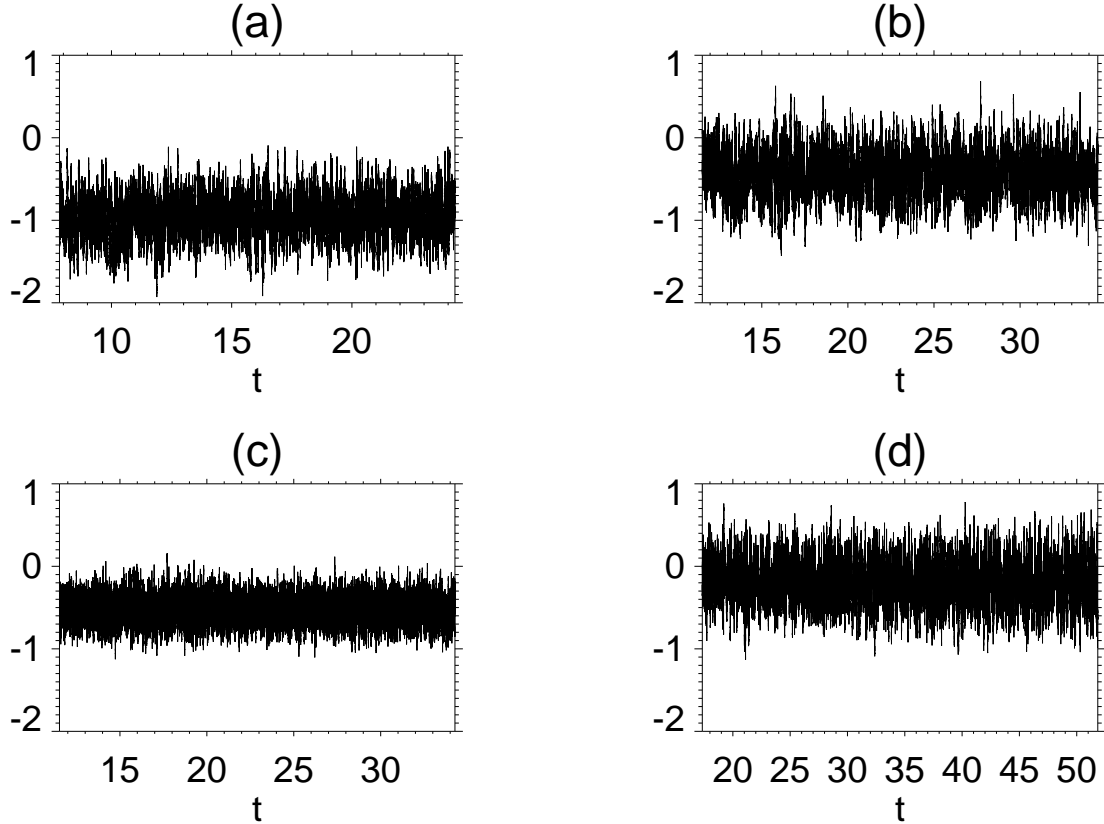


FIGURE 1. Timeseries of the electromotive force \mathcal{E} for short-correlation time flows with no shear. Here we consider flows (a) C_0 , (b) B_0 , (c) E_0 and (d) A_0 .

notation Run_{V_0} to represent the flow Run in table 1, to which a shear of strength V_0 is added. For example A_0 represents flow A from table 1 with no shear added, whilst F_{20} represents flow F from table 1 to which a shear of $V_0 = 20$ is added.

Figure 1 shows sample timeseries of the emf for a range of short-correlation time flows (with no imposed shear flow — so $V_0 = 0$). The emf is characterised by a well-defined mean with fluctuations about that mean that occur on a timescale comparable with the correlation time of the eddies. In figure 1(a) eddies on all scales from $k = 8$ to $k = 100$ contribute to the emf; we note here that $Rm(8) \approx 500$ whilst $Rm(100) \approx 15$ for our choice of η . In (b) and (c) the large and small scales contribute separately; we can compare the independence of the emf generation at various scales by comparing the distributions for the emf from the full spectrum to those calculated when the small and large scales are considered separately; this we do in the next subsection. It is also noticeable that the large-scale flows and small-scale flows have similar mean emfs, but the range (and also variance) of the emf from flows on the small scale is smaller. Thus the smaller scales are capable of contributing significant mean emfs with tighter distributions than the large-scale flows. This will be quantified in subsection 3.3. Finally (d) shows the emf for a case that only contains the very largest scales ($8 \leq k \leq 20$). These have a small mean and very large variance, a result which is in accord with arguments proposed above. Figure 2 shows that this behaviour persists for flows with moderate correlation times. Here the

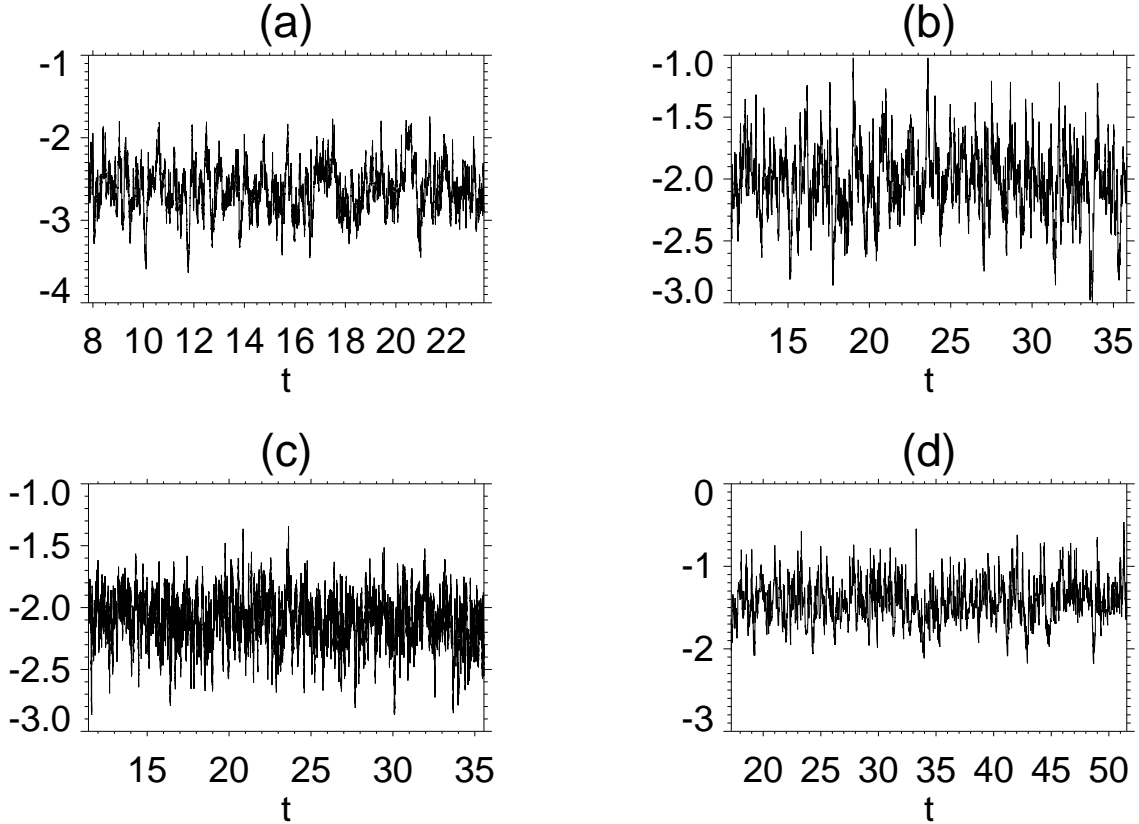


FIGURE 2. Timeseries of the electromotive force \mathcal{E} for moderate-correlation time flows with no shear. Here we consider flows (a) H_0 , (b) G_0 , (c) J_0 and (d) F_0 .

mean emfs are larger than for the comparable flows with short correlation times, but the picture remains that smaller spatial scales are capable of contributing to the mean emf without significantly affecting the variance. Recall here that the smaller scales are at smaller local magnetic Reynolds number $Rm(k)$.

Figures 3 and 4 show the comparable timeseries for the cases when a strong shear is included for both short and moderate correlation time flows. In all cases the shear has acted to reduce both the amplitude of the mean emf and, perhaps more significantly, the fluctuations about that mean. Shear this strong is able to act to modify the emf produced even by the flows on small-scales. A quantification of this effect is included in subsection 3.3

3.2. Contributions to the emf from different scales and their independence

In this subsection we quantify the role of different scales in determining the emf. In particular we examine which scales are responsible for generating a significant mean emf, and which lead to strong fluctuations about that mean. In order to be able to make such statements it is necessary to determine the degree of independence of the different scales in the flow in their contribution to the flow. We achieve this by utilising the following procedure: we consider three flows; one comprises eddies at only large scales, one only at small scales and one has both large and small-scale components. We then determine the distributions of the emf for these flows which we term emf_l (the emf for the large-

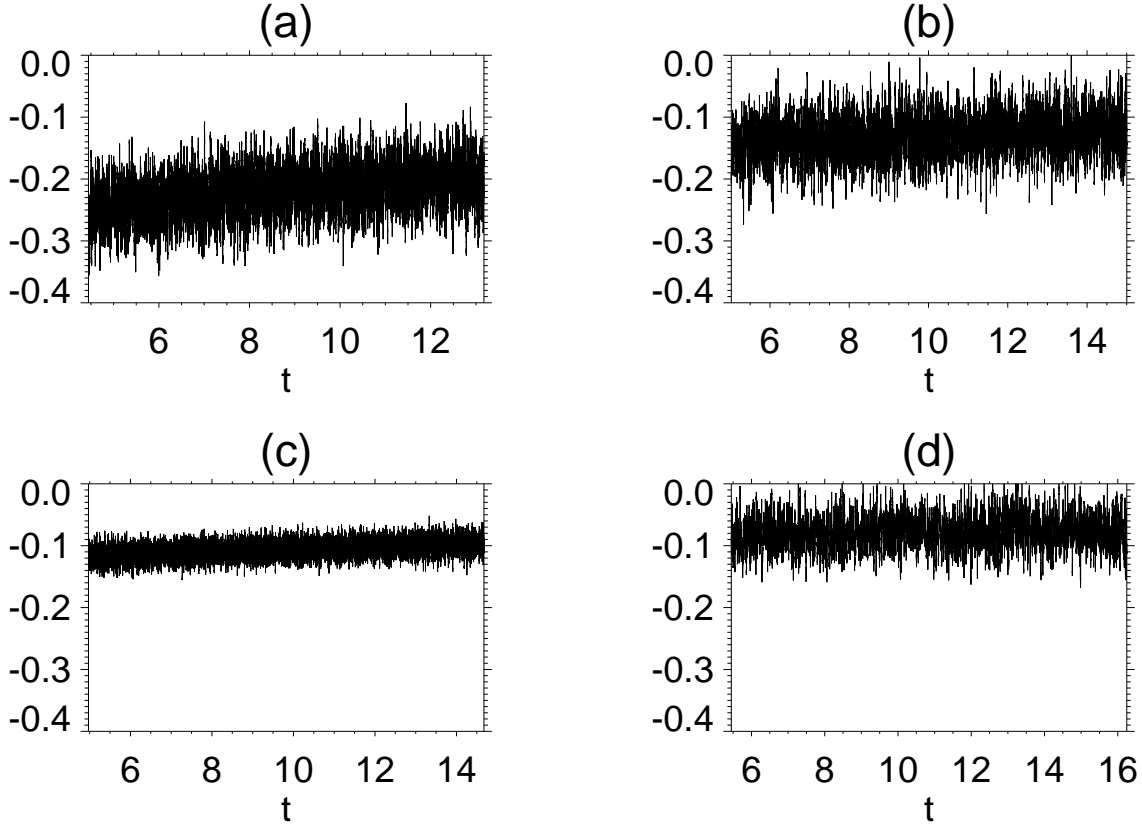


FIGURE 3. Timeseries of the electromotive force \mathcal{E} for short-correlation time flows with strong shear. Here we consider flows (a) C_{20} , (b) B_{20} , (c) E_{20} and (d) A_{20} .

scale flow) emf_s (the emf for the small-scale flow) and emf_a (the emf for the flow with all components). These emfs are shown in Figure 5 for the short correlation time flow, both in the presence and absence of large-scale shear. A number of points may be made immediately. For these flows it appears as though the large and small scales separately produce similar mean emfs to each other. However the fluctuations about this mean (as measured say by the variance of the the distributions) are significantly larger for the flows at large scales than those at small scales. The flow which has energy both at large and small scales produces more mean emf, but the variance of the emf is dominated largely by fluctuations driven by the large-scales (the variance does not differ significantly from that of the large-scale flow). The above statements are true both in the presence and absence of shear — the overall effect of the shear is in this case to reduce both the mean and the variance of the distributions for the emf, as will be discussed in the next section. Figure 6 shows the corresponding distributions for the flows with longer correlation time. Here the striking feature is the significant effect of the shear flow on both the mean and variance of the emf; the shear has had a significant effect in damping the emf of all scales; we shall also see that the presence of a strong shear here had made the scales less independent.

We proceed in calculating the independence of the scales, by examining the distribution emf_a and comparing it with the distribution of the variable which is the sum of the two

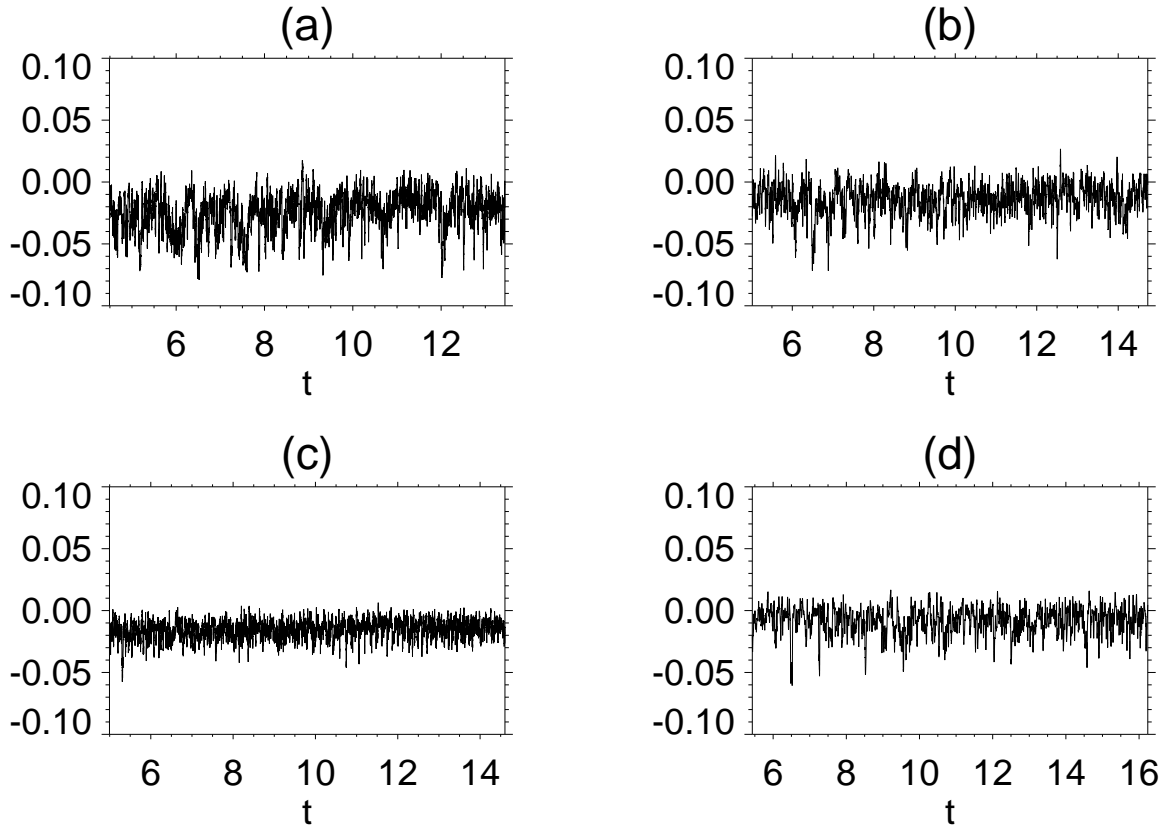


FIGURE 4. Timeseries of the electromotive force \mathcal{E} for moderate-correlation time flows with strong shear. Here we consider flows (a) H_{20} , (b) G_{20} , (c) J_{20} and (d) F_{20} .

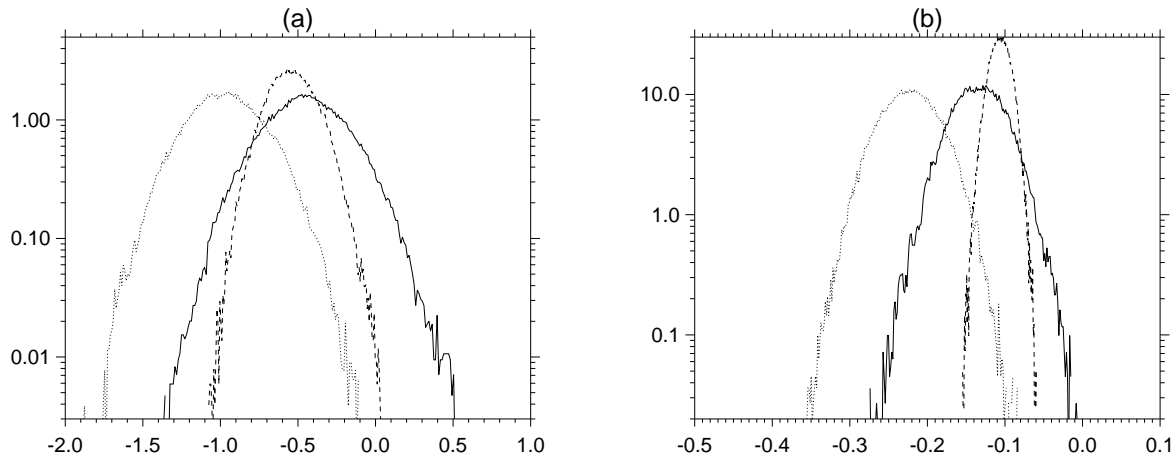


FIGURE 5. Distributions of emf at short correlation time for (a) cases with no shear B_0 (solid) E_0 (dashed) and C_0 (dotted) and (b) cases with strong shear B_{20} (solid) E_{20} (dashed) and C_{20} (dotted)

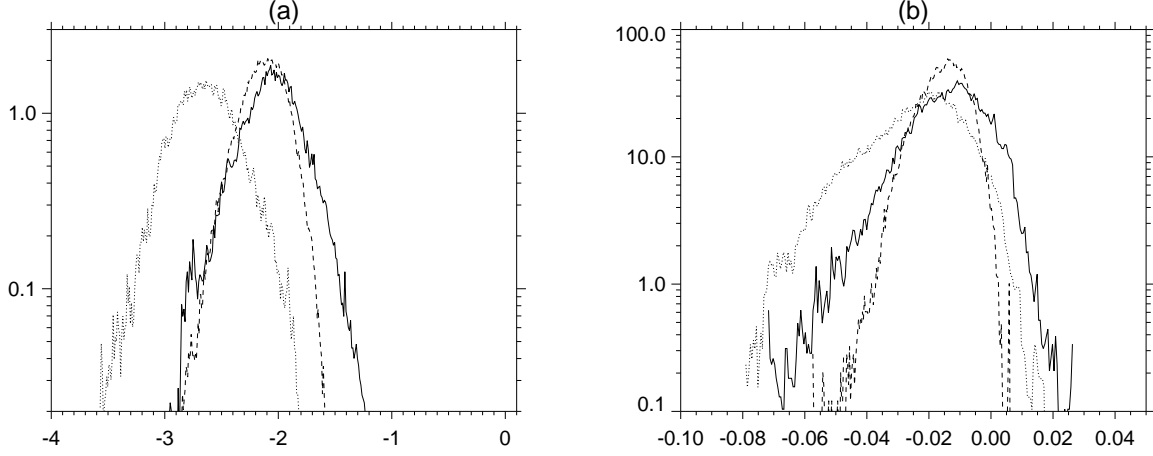


FIGURE 6. Distributions of emf at long correlation time for (a) cases with no shear G_0 (solid) J_0 (dashed) and H_0 (dotted) and (b) cases with strong shear G_{20} (solid) J_{20} (dashed) and H_{20} (dotted)

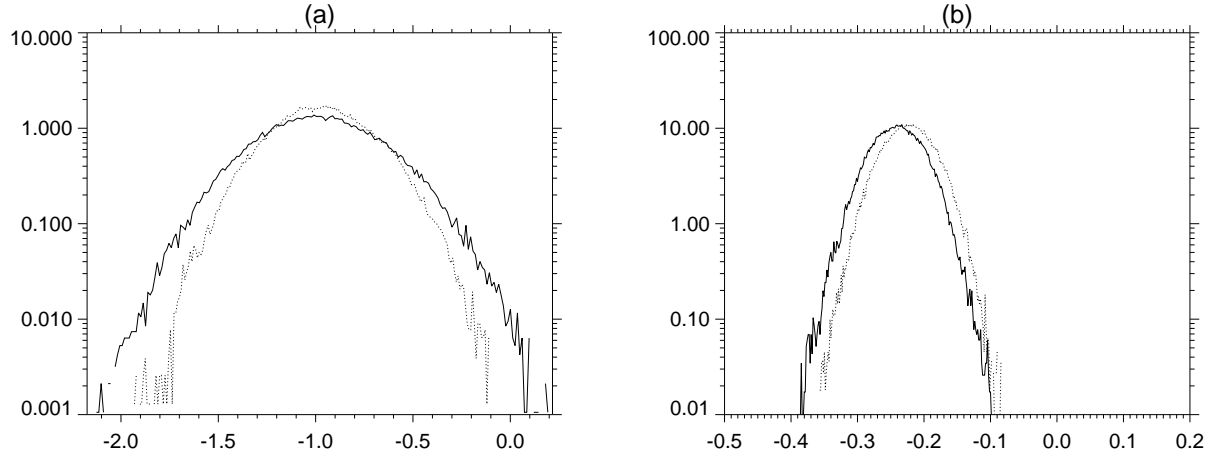


FIGURE 7. Distributions of the EMF for short correlation time flows: (a) cases C_0 (dotted) and E_0+B_0 (solid), (b) cases C_{20} (dotted) and $E_{20}+B_{20}$ (solid)

emfs (emf_s and emf_l).[†] If the large scales and small scales are acting independently then these distributions should be the same. Figure 7 compares these distributions for the short correlation time flows. The distributions are extremely similar, both with and without shear, which suggests that for these flows the scales are contributing to the emf independently — this is perhaps not surprising, owing to the rapid timescale on which the flows decorrelate (even at larger scales). The situation is similar in the presence of strong shear. However for longer correlation time flows, in the absence of shear, the contributions to the emf may not be independent as shown in Figure 8, which shows that the distributions are very different. This dependence is presumably a consequence of the larger scales which have the longest correlation times generating field that is acted

[†] An alternative procedure that yields the same results is to compare the distribution emf_a with that for the convolution of emf_l and emf_s .

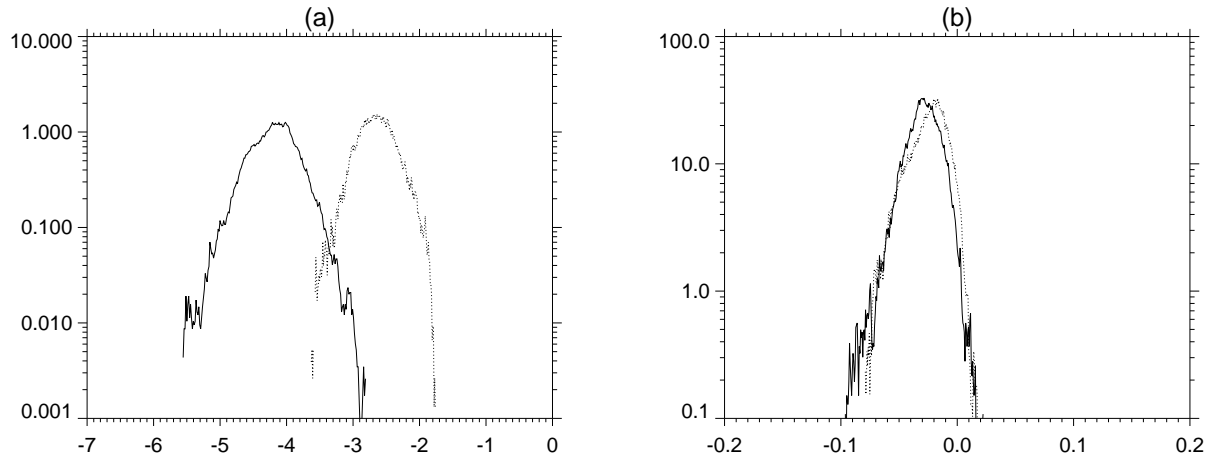


FIGURE 8. Distributions of the EMF for long correlation time flows: (a) cases H_0 (dotted) and J_0+G_0 (solid), (b) cases H_{20} (dotted) and $J_{20}+G_{20}$ (solid)

on by the smaller scales. Interestingly independence is re-established for these longer correlation time flows in the presence of strong shear as shown in Figure 8(b)

3.3. The role of shear, scaling of mean emf and the fluctuations

It is clear from the considerations of the previous sections that for flows with energy at large or small scales (or both large and small scales) the distribution of the emf is a function of the applied mean shear. This appears to be true both for short-correlation time flows and long-correlation time flows. Here we quantify the dependence of the first two moments of the distribution on the mean imposed shear.

Figure 9 shows these moments as a function of $(1 + V_0^2)$ on a *log-log* plot. The top two panels are for short correlation time flows. The left of these panels shows that for these flows, the contribution to the mean emf comes from both large and small scales for all values of the shear. For weak shears the mean emf is only weakly affected by the shear (with a slight decrease in the amplitude of the mean). At stronger shear rates the mean is significantly reduced. In contrast the variance is dominated by the large-scale flows (as noted earlier); the green curve tracks the black closely. The effect of shear on the variance is more pronounced with an immediate decrease of the variance even for small shear rates. Thus for small shear rates although the mean remains largely unaffected, the fluctuations about that mean are suppressed by the shear and the distribution of the emf is narrowed.

For flows with longer correlation times (bottom two panels), there are some similarities and differences. Again there appears to be equal contributions to the mean emf from the small and large-scale flows, but in this case (and in contrast to the short correlation time flows) the shear does have a significant effect even for small V_0 . The variance of the emf is again dominated by large-scale flows, and is again suppressed for even weak shears. Hence in this case both the mean emf *and* the fluctuations about that mean are reduced.

We conclude this section by fitting the dependence of the moments on the shear rate. For small shear rates this is clearly a strong function of the correlation time of the flows and so no universal fitting can be applied. We find that for large shears the scalings

$$\mu_{emf} \propto (1 + V_0^2)^{-\lambda}; \quad \sigma_{emf}^2 \propto (1 + V_0^2)^{-\kappa} \quad (3.1)$$

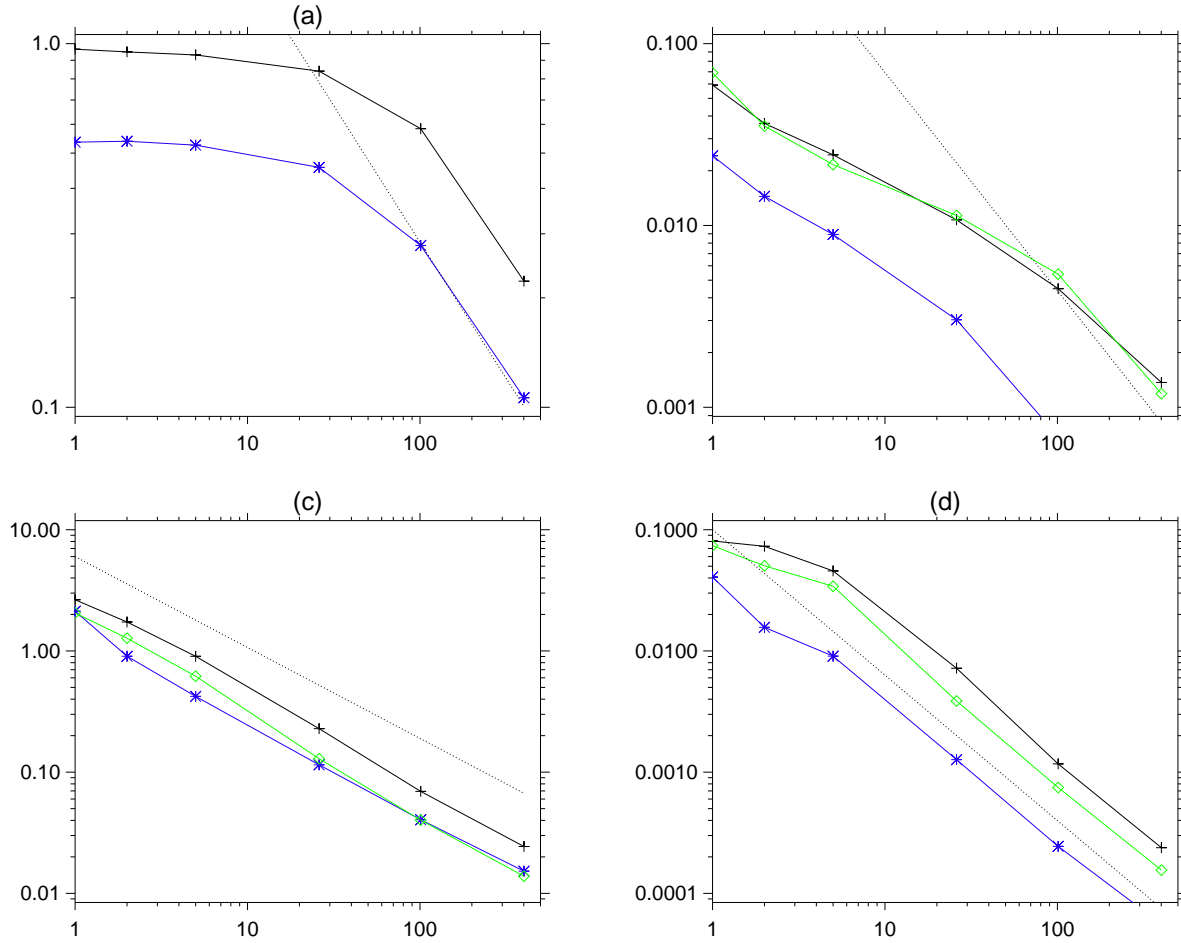


FIGURE 9. Moments of emf versus $(1 + V_0^2)$. (a) Amplitude of the mean emf for short correlation time flows for cases C (all scales; black), B (large scales; green) and E (small scales; blue) (b) Variance of emf for same cases. (c) Amplitude of the mean emf for long correlation time flows for cases H (all scales; black), G (large scales; green) and J (small scales; blue) (d) Variance of emf for same cases.

are consistent with the results for both long and short correlation time flows, with $\lambda \approx 0.75$ and $\kappa \approx 1.2$. The sensitivity of the variance to the strength of the shear is a key result, which can be used to interpret the dynamo's tendency to suppress fluctuations in the presence of shear (as discussed in the conclusion below).

4. Conclusion

In this paper we have examined the generation of the electromotive force (emf) by multi-scale random flows. The emf has a distribution with well-defined moments (such as mean and variance) that depend on the spatial scales contained in the flow and the strength of the systematic large-scale shear flow. We have shown that scales act more independently in generating the emf in short correlation time flows than in long correlation time flows in the absence of shear. The presence of shear tends to make the scales act more independently for both short and long correlation times.

An important result is that the mean emf and the fluctuations about that mean arise from different scales of the prescribed flow. Whereas all scales may contribute to the mean emf, the large spatial scales consistently contribute more to the variance of the distribution. The role of shear in modifying the distribution of the emf is also different for short and long correlation time flows. For short correlation time flows, the mean emf is only weakly dependent on shear rate; whilst for longer correlation time flows, the mean emf is much more sensitive to the shear rate. We therefore believe that it is dangerous to extrapolate from short correlation times to long correlation times when considering the likely distributions of the emf. We note that for both cases (long and short correlation time) the variance of the distribution of the emf is sensitive to the strength of the shear.

We conclude by speculating on the importance of these results for large and small scale dynamo action. It is tempting to identify the mean emf with a tendency of the resulting dynamo to produce large-scale fields, whereas fluctuations in the emf about that mean may be identified with small-scale dynamos. If this is the case then both large and small-scale flows are able to contribute to the large-scale dynamo, large-scales (which are at higher Rm) contribute more to the small scale dynamo. This is consistent with the theory proposed by Tobias & Cattaneo (2008a). Moreover the small-scale dynamo is more sensitive than the large-scale dynamo to presence of shear. It is therefore plausible, as suggested by Tobias & Cattaneo (2013) Cattaneo & Tobias (2014) that the primary effect of the presence of shear at high Rm may be to suppress small-scale dynamo action whilst allowing the large-scale dynamo to manifest itself.

We conclude by discussing what is meant by a dynamo operating at high Rm . Clearly large Rm can mean different things to different authors, and simply quoting a value of Rm may be misleading. Two crucial values of Rm can easily be identified in the kinematic regime. The first of these Rm_c is the critical value of Rm at which dynamo action sets in. The second Rm_a is that value at which the growth-rate of the flow approaches its asymptotic limit (for practical purposes this could be defined as coming with 5% of this limit). Typically $Rm_a \gg Rm_c$ and is not usually accessible to three-dimensional calculations. Even for the Galloway-Proctor flow $Rm_a \approx 50Rm_c$, and it is only the fact that the calculation is quasi two-dimensional that allows access to magnetic Reynolds numbers greater than Rm_a . We recognise that calculation of Rm_a is difficult in fully three-dimensional calculations, but we argue here that it is incumbent on dynamo theorists to provide the value of $\chi = (Rm - Rm_c)/Rm_c$ for their calculations so it is possible to evaluate whether their calculations may be close to asymptotic. Typically this value would need to be $\chi \sim \mathcal{O}(100)$ before any claims of high Rm should be made. We note that these calculations are performed with $\chi \sim 250$ and so can be regarded as being at high Rm .

Acknowledgements: SMT would like to thank STFC for funding.

REFERENCES

- AUGUSTSON, K., BRUN, A. S., MIESCH, M. & TOOMRE, J. 2014 Grand Minima and Equatorward Propagation in a Cycling Stellar Convective Dynamo. *ArXiv e-prints* .
- BOLDYREV, S., CATTANEO, F. & ROSNER, R. 2005 Magnetic-Field Generation in Helical Turbulence. *Physical Review Letters* **95** (25), 255001–+.
- BRANDENBURG, A. & SUBRAMANIAN, K. 2005 Astrophysical magnetic fields and nonlinear dynamo theory. *Physics Reports* **417**, 1–209.
- CATTANEO, F. & TOBIAS, S. M. 2005 Interaction between dynamos at different scales. *Physics of Fluids* **17** (12), 127105.

- CATTANEO, F. & TOBIAS, S. M. 2014 On Large-scale Dynamo Action at High Magnetic Reynolds Number. *Astrophysical Journal* **789**, 70.
- CHILDRESS, S. & GILBERT, A. D. 1995 *Stretch, Twist, Fold*.
- COURVOISIER, A., HUGHES, D. W. & TOBIAS, S. M. 2006 α Effect in a Family of Chaotic Flows. *Physical Review Letters* **96** (3), 034503.
- COURVOISIER, A. & KIM, E.-J. 2009 Kinematic α effect in the presence of a large-scale motion. *Phys. Rev. E* **80** (4), 046308.
- COWLING, T. G. 1933 The magnetic field of sunspots. *Mon. Not. Roy. Ast. Soc.* **94**, 39–48.
- FINN, J. M. & OTT, E. 1988 Chaotic flows and fast magnetic dynamos. *Physics of Fluids* **31**, 2992–3011.
- GALLOWAY, D. J. & PROCTOR, M. R. E. 1992 Numerical calculations of fast dynamos in smooth velocity fields with realistic diffusion. *Nature* **356**, 691–693.
- HARGITTAI, I. 2013 *Buried Glory: Portraits of Soviet Scientists*. Oxford University Press.
- KÄPYLÄ, P. J., KORPI, M. J. & BRANDENBURG, A. 2010 The α effect in rotating convection with sinusoidal shear. *Mon. Not. Roy. Ast. Soc.* **402**, 1458–1466.
- KRAUSE, F. & RAEDLER, K. H. 1980 *Mean-field magnetohydrodynamics and dynamo theory*. Oxford, Pergamon Press.
- MOFFATT, H. K. 1978 *Magnetic field generation in electrically conducting fluids*. Cambridge, England, Cambridge University Press, 1978. 353 p.
- PLUNIAN, F. & RÄDLER, K.-H. 2002 Subharmonic Dynamo Action in the Roberts Flow. *Geophysical and Astrophysical Fluid Dynamics* **96**, 115–133.
- ROBERTS, G. O. 1972 Dynamo action of fluid motions with two-dimensional periodicity. *Phil. Trans. Roy. Soc. Lond. A* **271**, 411–454.
- STEENBECK, M., KRAUSE, F. & RÄDLER, K.-H. 1966 Berechnung der mittleren LORENTZ-Feldstärke für ein elektrisch leitendes Medium in turbulenter, durch CORIOLIS-Kräfte beeinflusster Bewegung. *Zeitschrift Naturforschung Teil A* **21**, 369.
- SUNYAEV, R. A. 2004 *Zeldovich reminiscences*.
- TOBIAS, S. M. & CATTANEO, F. 2008a Dynamo action in complex flows: the quick and the fast. *Journal of Fluid Mechanics* **601** (-1), 101–122.
- TOBIAS, S. M. & CATTANEO, F. 2008b Limited Role of Spectra in Dynamo Theory: Coherent versus Random Dynamos. *Physical Review Letters* **101** (12), 125003–+.
- TOBIAS, S. M. & CATTANEO, F. 2013 Shear-driven dynamo waves at high magnetic Reynolds number. *Nature* **497**, 463–465.
- TOBIAS, STEVEN M., CATTANEO, FAUSTO & BOLDYREV, STANISLAV 2011 MHD Dynamos and Turbulence .
- TOBIAS, S. M., CATTANEO, F. & BRUMMELL, N. H. 2008 Convective Dynamos with Penetration, Rotation, and Shear. *Astrophysical Journal* **685**, 596–605.
- VAINSHTAIN, S. I. & KICHATINOV, L. L. 1986 The dynamics of magnetic fields in a highly conducting turbulent medium and the generalized Kolmogorov-Fokker-Planck equations. *Journal of Fluid Mechanics* **168**, 73–87.
- ZEL'DOVICH, YA. B. 1957 The magnetic field in the two-dimensional motion of a conducting turbulent fluid. *Sov. Phys. JETP* **4**, 460–462.